Modelling an ammonia cycle for thermochemical energy storage

A. García-Guzmán[a], D. A Rodríguez Pastor[b], J. A Becerra[c] and R.Chacartegui[d]

[a] *University of Seville, Seville, Spain, alejandrogarciaguzman10@gmail.com*
[b] *University of Seville, Seville, Spain, drodriguez4@us.es*
[c] *University of Seville, Seville, Spain, jabv@us.es*
[d] *University of Seville, Seville, Spain, ricardoch@us.es*

Abstract:
The penetration of renewable energies into the electricity system is making it increasingly cheaper, cleaner, and safer. It poses specific challenges, such as dispatchability periods and grid frequency stability.
Storage systems are needed to meet these challenges. Thermochemical reactions have great potential for energy transport and storage. Their integration into solar energy systems is of great interest due to the possibility of achieving high energy densities and seasonal storage. This work analyses the integration of a thermochemical storage system based on ammonia looping into a concentrating solar power (CSP). Energy storage is based on a charging phase, where heat is provided for ammonia decomposition and a discharging phase, where heat is recovered from ammonia synthesis. This work aims to evaluate the thermodynamic performance of a reference plant with a total capacity of 6.2 MW of CSP integrated into an ammonia loop power system. The performance and LCOS curves are discussed as a function of synthesis and decomposition temperatures.

Keywords:
TCES, Ammonia looping, CSP, Thermochemical energy storage

1. Introduction

Energy storage systems are used to ensure the availability of energy supply. Thermal energy storage (TES) and Thermochemical energy storage (TCES) systems are promising technologies for renewable energy storage [1]. In recent years, several thermal storage technologies for medium- and high-temperature CSP systems have been developed based on the use of materials in which energy is stored as sensible heat [1]–[5] or latent heat [6].The third form of storage is through thermochemical storage, in which the heat from the sun drives an endothermic reaction, which decomposes a compound into other species, storing the energy in chemical bonds. This has the advantage that it can be used for long-term energy storage. Different thermochemical energy storage approaches have promising results[7]–[9] based on the methanol decomposition into syngas [10] or iron carbonates [11].

They have an optimum operation at different temperature levels, offering solutions to efficiently convert, store and transport solar energy. They allow seasonal storage capacity allowing long mismatch between resource availability and discharge for covering demand. Depending on the involved reactions, they can have high energy densities [12]. The thermochemical energy storage system based on the ammonia looping is based on the decomposition and synthesis of the pair NH_3/H_2. It has an energy density of 131 MJ/m^3 with a turning temperature of 195 ºC [7] [11]. From the point of view of thermochemical storage, the reactions of synthesis and decomposition of ammonia are opposite reactions that share the absorption and desorption of dinitrogen stage.

Ammonia is a carbon-free hydrogen carrier with a reasonably good volumetric and gravimetric energy density compared to hydrogen. It has an energy density of 13.1 GJ/m, whereas hydrogen has an energy density of 3.5 GJ/m [13], and it is used as a feedstock and raw material to produce other chemicals [14].

The ammonia chemical industry has a high environmental impact and needs the integration of renewable energy to reduce it [15]. There are several possibilities for integrating renewables in the ammonia industry: using biomass gasification systems [16]–[18], solar energy [19], [20], and wind energy [21], [22]. Another option is to use biogas produced from the decomposition of organic material, such as agricultural waste or animal excrement [23], as a source of hydrogen.

https://doi.org/10.52202/069564-0199

Ammonia-based solar thermochemical storage systems can help ensure the stability of solar thermal power generation systems 24-h basis, offering a high potential for long-term energy storage. Besides, ammonia, the main raw material for fertiliser production, can be integrated into a thermochemical storage system. *Carden et al.* pioneered the idea of the ammonia-based energy storage system in 1974 [24]. Subsequent exergy analyses studies conducted concluded that the main irreversibility is the heat recovery process. The main losses are concentrated in the reaction, the heat transfer within the exothermic reactor and the losses of the exothermic reactor countercurrent heat exchanger[25]. In 2019, *Chen et al.* [26] studied the effects of dissociation reactor geometry by performing a 2-dimensional pseudo-homogeneous cylindrical 2-dimensional model of a dissociation reactor, concluding that converging conical reactors can achieve the highest conversions. *Lovegrove et al.* proposed an ammonia looping system which operates at a nominal power level of 1 kW_{chem} solar dissociation reactor kW_e [27], [28].

This work proposes a novel and flexible system in which the renewable energy produced by the sun can be stored for a long time. Subsequently, this stored energy is released in the form of heat. This can be used for power generation or to provide heat to a process. It is a carbon-free process where ammonia is produced based on renewables [29]–[31], thus reducing the consumption of fossil fuels. The efficient and simple form of the system results in a competitive levelised cost of storage.

2. System description

The system consists of a charging cycle, where the ammonia decomposition reaction is carried out, and a discharge cycle, where the ammonia synthesis reaction is carried out. The concentrating solar power and a heliostat field are integrated into the charge phase to generate syngas through endothermic decomposition. In the discharge phase, the syngas is released to the synthesis phase and is converted into ammonia, releasing heat to a power cycle.

In the charging phase, ammonia is stored at 30°C and 25 bar and released to a pump that raises the pressure to 100 bar. The ammonia is preheated with the outlet of the decomposition reactor. This ammonia feeds the endothermic reactor at 382.3 ºC and 100 bar. The outlet of the reactor contains syngas and unreacted ammonia at 500 ºC and 100 bar[13], [32]–[34]. This outlet stream is cooled with the ammonia inlet to the reactor to 94.31 ºC.

Figure 1. Conceptual process flow diagram of the ammonia cycle system

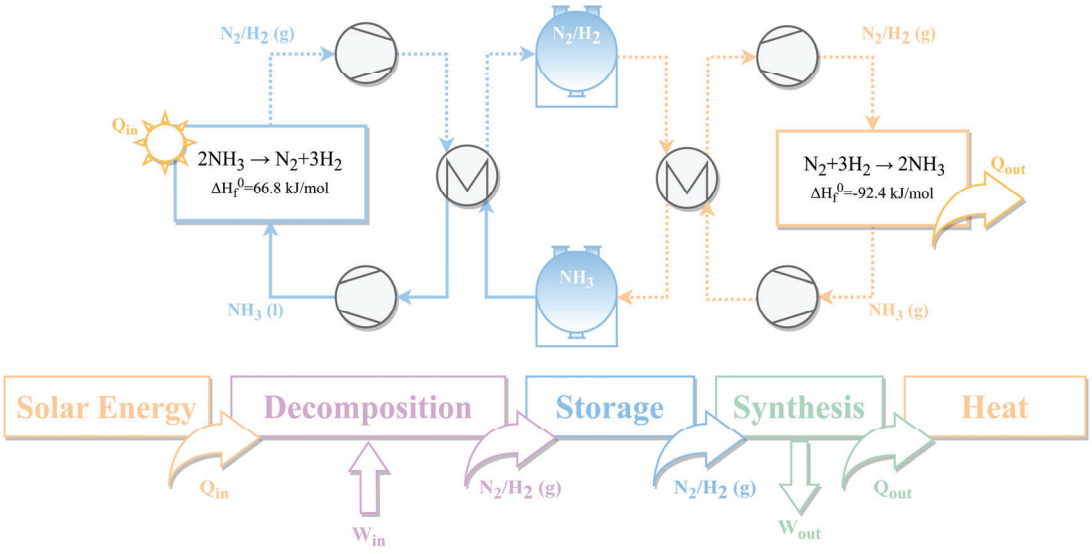

https://doi.org/10.52202/069564-0199

Figure 2. Process flow diagram of the ammonia cycle system

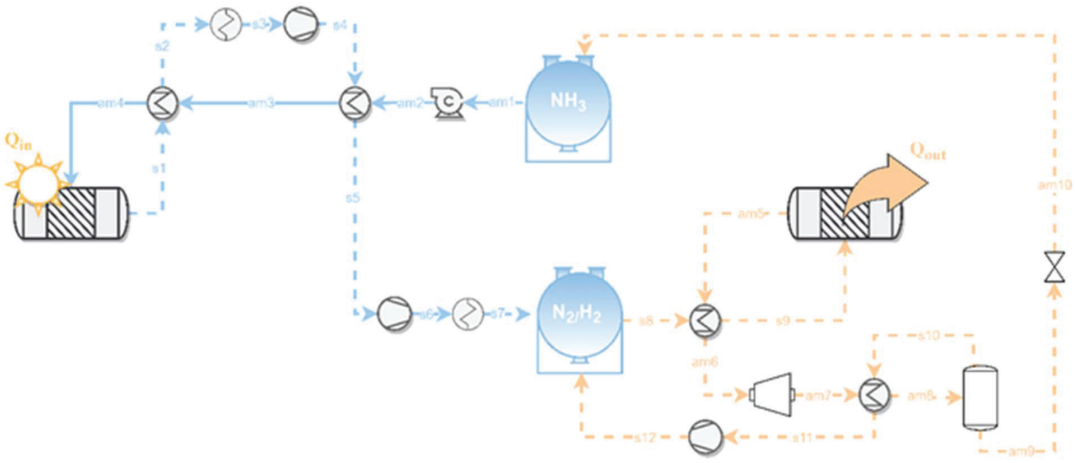

In the loading phase, ammonia is stored at 30°C and 25 bar and released to a pump that raises the pressure to 100 bar. The ammonia is preheated with the outlet of the decomposition reactor. This ammonia feeds the endothermic reactor at 382.3 ºC and 100 bar. The reactor outlet contains syngas and unreacted ammonia at 600 ºC and 100 bar. This outlet stream is cooled with the ammonia inlet to the reactor to 94.31 ºC and raises its pressure to 200 bar. Then, the syngas at 200 bar is stored [35].

Figure 3. Process flow diagram of the ammonia decomposition (charge phase)

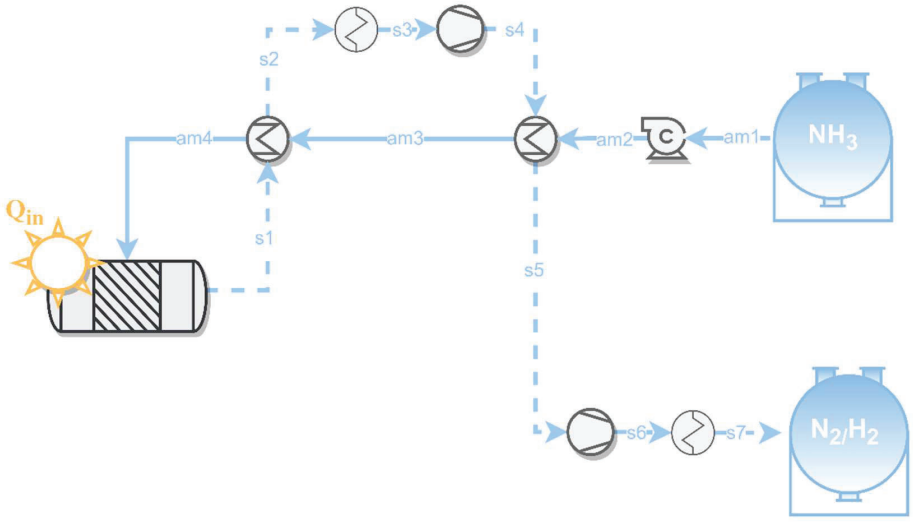

In the discharge phase, the synthesis gas is released from the tank, and this stream is cooled with the reactor outlet. The inlet stream to the synthesis reactor is at 189.4 °C and 200 bar [36] with a catalyst converter Ba/Ru/BN [35]. The reactor outlet stream is at 300 ºC and 200 bar [36]. It separates in a flash into ammonia and unreacted synthesis gas. At a steady state and with a sufficiently long residence time in the reactor, the syngas would tend to be zero in the synthesis reactor outlet stream.

https://doi.org/10.52202/069564-0199

Figure 4. Process flow diagram of the ammonia synthesis (discharge phase)

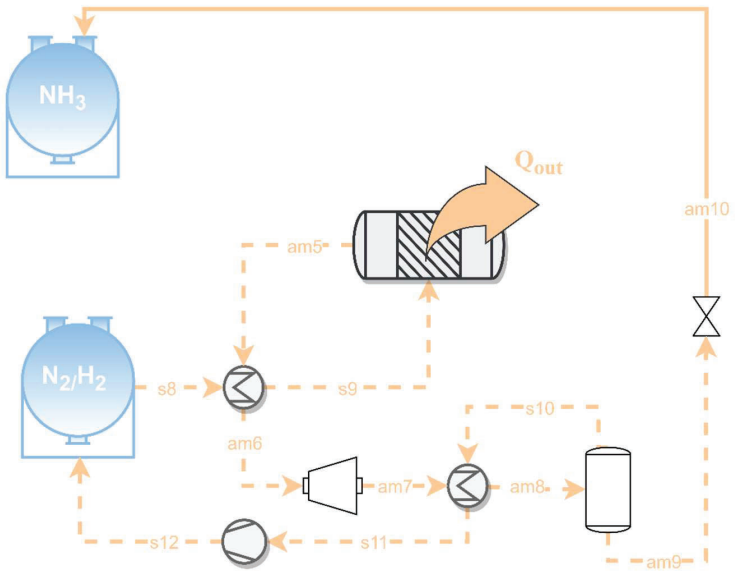

3. Simulation

In this section, simulations of the proposed system layout will be carried out. These simulations will be carried out in the Aspen Hysys commercial software.

A series of operating conditions were previously defined to simulate the model, both in the loading and discharging phases.

a. Steady-state model.
b. Sufficient residence time to achieve an overall conversion of 100%.
c. The minimum approach temperature for all heat exchangers is 20 ºC.
d. The efficiencies of the pumps, compressors and turbines are 80, 89, and 90%, respectively.
e. The global, solar-to-chemical and solar-to-electric efficiencies have been defined according to equations 1, 2 and 3.

Table 1. Main parameters of the plant

Parameter	Value	Unit
NH_3 storage temperature/pressure	30/25	ºC/bar
Syngas CO/H2 storage pressure	200	bar
Endothermic reaction temperature/pressure	500/100	ºC/bar
Exothermic reaction temperature/pressure	250/200	ºC/bar
Inlet NH_3 molar flow of the charging process	100	mol/s

The global performance of the plant is defined as follows.

https://doi.org/10.52202/069564-0199

$$\eta_{plant} = \frac{\dot{Q_{exo}} + \dot{W_T}}{HH\dot{V}_{NH_3}\dot{m_{NH_3}} + \dot{W_C} + \dot{Q_{CSP}}} * \frac{h_{discharge}}{h_{charge}} \quad [1]$$

The numerator represents the outputs, which are the energy extracted from the ammonia synthesis and the power generated by the expansion turbines, while the denominator represents the heat flow of the ammonia stream from the synthesis reactor outlet, the energy consumption by the compressors and the pump, and the heat supplied by the CSP. This is affected by a ratio of discharge hours to charge hours.

Also, equations [2] and [3] define a solar-chemical yield and a solar-electric yield. The former represents the thermal recovery of the dissociation reaction compared to the CSP power input, while the solar-electric yield represents the electrical energy recovery compared to the CSP power and the energy consumption of the compressors and pump. Both efficiencies are in terms of heat and electrical energy, respectively.

$$\eta_{sol-ch=} \frac{X_{NH_3} m_{NH_3} \Delta h_{NH_3}}{\dot{Q_{CSP}}} \quad [2]$$

$$\eta_{sol-elec} = \frac{\dot{W_T}}{\dot{W_C} + \dot{Q_{CSP}}} \quad [3]$$

3.1 Economic model

The technical-economic analysis was carried out by evaluating the CAPEX and OPEX and then evaluating the LCOS of the system.

The levelized cost of storage (LCOS) according to equation 4.

$$LCOS = \frac{CAPEX + \sum_{i=1}^{n} \frac{OPEX}{(1+r)^n}}{\sum_{i=1}^{n} \frac{Qexo}{(1+r)^n}} \quad [4]$$

It is assumed a discount rate (r) of 3% and a useful life of the plant (n) of 20 years.

The CAPEX was evaluated using equipment costs. These equipment costs are calculated based on the correlations shown in **Table 2**. OPEX is assumed to be 20% of CAPEX.

Table 2. Correlations for estimating equipment costs.

Equipment	Scaling parameter	Expression	Reference
Pump	Brake power [kW] and isentropic efficiency	$IC_C = 6898 \cdot \dot{W}_{Compressor}^{0.7865}$	[37]
Compressor	Power [kW]	$IC_P = 750 \cdot (\dot{W}_p)^{0.71} \cdot \left[1 + \left(\frac{0.2}{1-\eta_{i,P}}\right)\right]$	[38]
Turbine	Power [kW]	$IC_T = 4001.4 \cdot \dot{W}_{Turbine}^{0.6897}$	[37]
Endotermic reactor	Power [kW]	$IC_{DR} = 193000 \cdot \dot{Q}_{endo}^{0.65}$	[39]

Exotermic reactor	Power [kW]	$IC_{SR} = 19594 \cdot \dot{Q}_{exo}^{0.5}$	[38]
Tank	Volume [m^3]	$C_{tank} = 83 \cdot V_{tank} \cdot 10^{-6}$	[40]
Heat exchangers	Exchanger Area [m^2] pressure [bar]	*Table*	[38]
Solar tower and receiver	$\Phi_{Receiver}\ [kW]$	$IC_{tower}^{solar} = 57.07 \cdot \Phi_{Receiver}$	[41]
Electric generator	Power [MW]	$IC_{EG} = 106 \cdot P_G^{0.95}$	[38]

4. Results

The results of the system at nominal conditions are shown in **Table 3**. The solar-to-chemical performance is high (>90 %) due to the high conversion achieved in the decomposition reactor regarding the power input by the sun. The global performance is low compared to other TCES, as expected by the temperature levels. However, it the LCOS is remarkable, which is fairly low compared to other technologies.

Table 3. Results at the operation point

Parameter	Value	Unit
Global performance	11.55	%
Solar to chemical performance	91.84	%
Solar to electrical performance	1.753	%
Exothermic reaction heat	-3.78	MW
Endothermic reaction heat	6.207	MW
CAPEX	3.964	M€
OPEX	0.793	M€
LCOS	63.98	€/MWh

It can be observed that the LCOS of the plant is 63.98 €/MWh, which is a competitive value, in comparison with other types of long-term thermochemical energy storage, such as H_2 and CH_4 storage with levelized cost of electricity of 260-430 €/MWh and 360-550 €/MWh, respectively. Table 4 shows the LCOS of the different technologies for long-term and short-term storage. [42]

Table 4. Comparison table of LCOS for the different technologies for long-term storage

Technology	Type of storage	LCOS [€/MWh]
PSH (Pumped Storage Hydroelectricity)	long-term	930-1850
dCAES (Diabatic Compressed Air Storage)	long-term	20
aCAES (Adiabatic Compressed Air Storage)	long-term	20-40
H_2 Storage	long-term	260-430
CH_4 storage	long-term	360-530
NH_3 storage	long-term	64

https://doi.org/10.52202/069564-0199

4.1. Sensitivity analysis

Different sensitivity analyses were performed as a function of endothermic temperature. **Figure 5** shows the effect of the molar fraction as a function of the decomposition temperature and synthesis temperature. As the decomposition temperature increases, the molar fraction of ammonia increases, whereas as the synthesis temperature increases, the conversion of ammonia to syngas decreases to a lesser extent than the decomposition reaction. These conversions justify performance trends.

Figure 5. Concentration profiles as a function of decomposition temperature (on the left) and synthesis temperature (on the right)

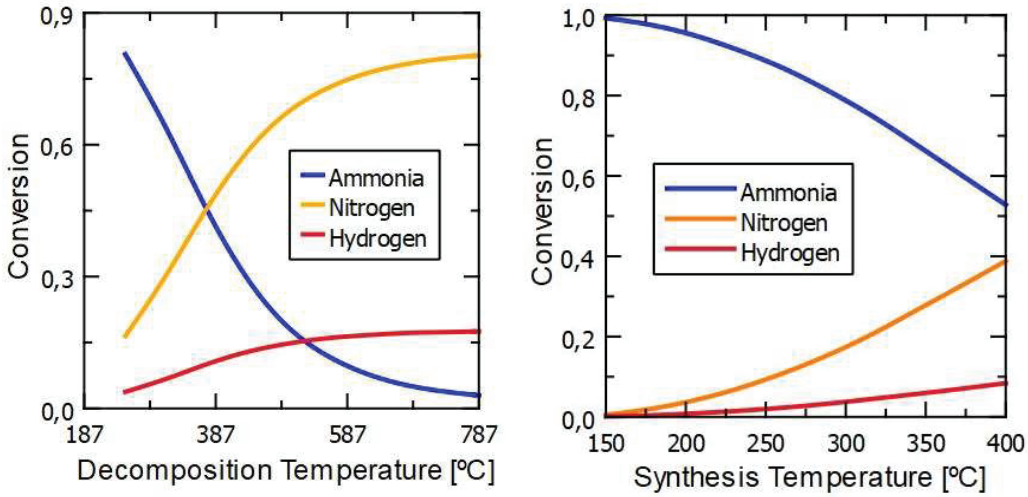

The next analysis is the global performance as a function of the decomposition and synthesis temperatures parametrised at four pressures. It has been shown that the higher the operating temperature, the higher the overall plant performance. Also, as operating pressures increase, lower overall plant performance. Increasing the endothermic temperature increases the conversion of ammonia to syngas, thus increasing the conversion in ammonia synthesis, releasing more heat of reaction, and increasing the yield. Likewise, the increase in pressure in the discharge phase increases the compression power, affecting the denominator and lowering the yield.

Figure 6 follows the same trend of the overall yield as a function of the decomposition temperature, but as the reaction temperature increases, the yield decreases. Increasing the reaction temperature the conversion decreases. Therefore, the heat flow of the reactor outlet stream is lower, affecting the numerator of the yield and decreasing it.

From these graphs, the optimum operating conditions that optimise the overall performance of the plant can be selected. The higher the decomposition temperature and the lower the synthesis temperature, the higher the overall plant performance.

https://doi.org/10.52202/069564-0199

Figure 6. Global performance as a function of decomposition temperature parametrised at four pressures (on the left) and parametrised at four synthesis temperatures.

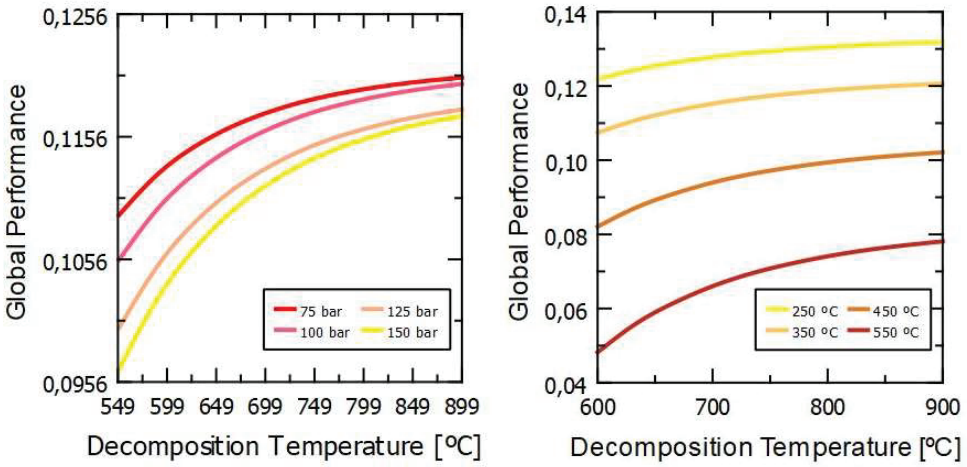

In figure 7 it is shown the exothermic heat release as a function of synthesis temperature parametrised at four decomposition temperatures. As a synthesis temperature increases, the exothermic heat released decreases. In the opposite trend, as the decomposition temperature increase, the heat releases increase. This fact is because as the decomposition temperature increases, the syngas produced is higher. Then, the conversion of syngas to ammonia in the synthesis reactor is greater, releasing more heat.

Figure 7. Exothermic heat release as a function of synthesis temperature parametrised at four decomposition temperatures.

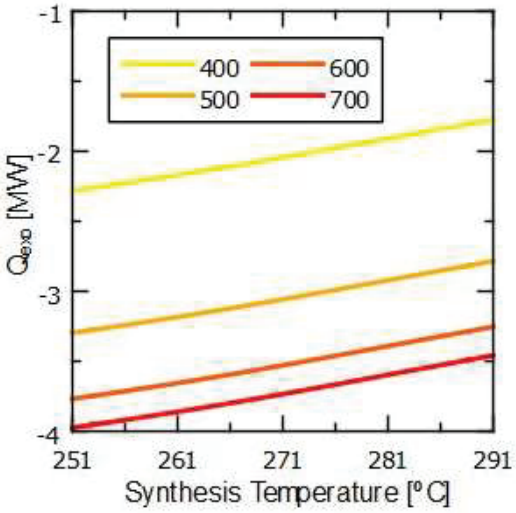

https://doi.org/10.52202/069564-0199

Figure 8 shows the levelized cost of storage as a function of the decomposition temperature and the synthesis temperature. As the decomposition temperature increases, the LCOS decreases. Likewise, as the synthesis temperature increases, the LCOS takes an opposite trend, decreasing.

Figure 8. LCOS as a function of decomposition temperature parametrised at four pressures (on the left) and synthesis temperature (on the right).

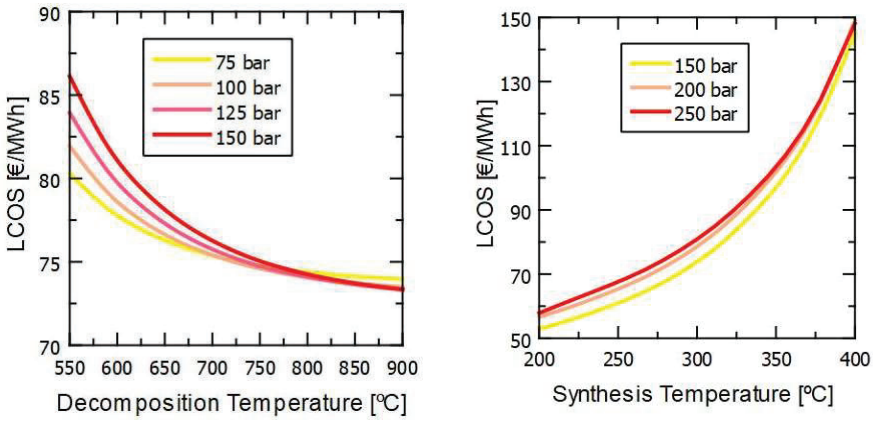

It is shown the higher the ammonia pressure at the reactor inlet, the higher the LCOS because the OPEX of the installation increases as the pressure drop in the pump increases. This trend is equal in the discharge phase.

When the decomposition temperature rises, the reaction is favoured and shifts to the right, producing more syngas. Then the heat released in the synthesis reactor will be higher. This increases the denominator of the LCOS by lowering it. As the synthesis temperature increases, the heat of reaction decreases, resulting in a rise in LCOS. The rise in the OPEX is reflected mainly in the pressure in both analyses. As the pressure increases, the LCOS increases.

5. Conclusions

A thermochemical storage system is proposed, based on the decomposition and synthesis of green ammonia, being a CO_2-free solution and a very dispatchable system in terms of energy production.

There are several advantages of the proposed system that can be mentioned.

i. The solar-to-chemical performance is high (92%) due to the high conversion of ammonia in the decomposition reaction. In contrast, the overall thermal efficiency of the system is 11.55%, which is low due to high compression consumption in relation to the exothermic energy generated in the synthesis reaction and the temperature levels.

ii. The system produces 3.78 MW of exothermic heat, with 6.2 MW of power input in the CSP, based on 100 mol/s of green ammonia.

iii. The system has a competitive LCOS value of 63.98 €/MWh for the design conditions. It is a competitive position concerning other long-term thermochemical systems storage, such as H_2 or CH_4 storage.

iv. The temperature/pressure torque for the load plus phase is 30ºC/25 bar, and for the discharge phase 250ºC/200 bar, making a compromise between overall plant performance and LCOS.

https://doi.org/10.52202/069564-0199

Acknowledgements

This work has been made possible thank to the project “Prueba de concepto en entorno relevante de nuevo diseño de calcinador solar de alta temperatura y elevada eficiencia”

Nomenclature

η efficiency, [-]

$\dot{Q}$ heat power, [kW]

$\dot{W}$ heat power, [kW]

X molar fraction [-]

$\dot{m}$ mass flow [kg/s]

Δh enthalpy difference, [kJ/kmol]

I_C Investment cost, [€]

References

[1] A. Gautam and R. P. Saini, “A review on sensible heat based packed bed solar thermal energy storage system for low temperature applications,” *Solar Energy*, vol. 207, pp. 937–956, Sep. 2020, doi: 10.1016/J.SOLENER.2020.07.027.

[2] G. Li, “Sensible heat thermal storage energy and exergy performance evaluations,” *Renewable and Sustainable Energy Reviews*, vol. 53, pp. 897–923, Jan. 2016, doi: 10.1016/J.RSER.2015.09.006.

[3] M. M. Sorour, “Performance of a small sensible heat energy storage unit,” *Energy Convers Manag*, vol. 28, no. 3, pp. 211–217, Jan. 1988, doi: 10.1016/0196-8904(88)90024-6.

[4] L. Seyitini, B. Belgasim, and C. C. Enweremadu, “Solid state sensible heat storage technology for industrial applications – A review,” *J Energy Storage*, vol. 62, p. 106919, Jun. 2023, doi: 10.1016/J.EST.2023.106919.

[5] L. Seyitini, B. Belgasim, and C. C. Enweremadu, “Solid state sensible heat storage technology for industrial applications – A review,” *J Energy Storage*, vol. 62, p. 106919, Jun. 2023, doi: 10.1016/J.EST.2023.106919.

[6] H. Jouhara, A. Żabnieńska-Góra, N. Khordehgah, D. Ahmad, and T. Lipinski, “Latent thermal energy storage technologies and applications: A review,” *International Journal of Thermofluids*, vol. 5–6, p. 100039, Aug. 2020, doi: 10.1016/J.IJFT.2020.100039.

[7] R. Chacartegui, A. Alovisio, C. Ortiz, J. M. Valverde, V. Verda, and J. A. Becerra, “Thermochemical energy storage of concentrated solar power by integration of the calcium looping process and a CO2 power cycle,” *Appl Energy*, vol. 173, pp. 589–605, Jul. 2016, doi: 10.1016/J.APENERGY.2016.04.053.

[8] A. Alovisio, R. Chacartegui, C. Ortiz, J. M. Valverde, and V. Verda, “Optimising the CSP-Calcium Looping integration for Thermochemical Energy Storage,” *Energy Convers Manag*, vol. 136, pp. 85–98, Mar. 2017, doi: 10.1016/J.ENCONMAN.2016.12.093.

[9] C. Ortiz, J. M. Valverde, R. Chacartegui, L. A. Perez-Maqueda, and P. Giménez, “The Calcium-Looping (CaCO3/CaO) process for thermochemical energy storage in Concentrating Solar Power plants,” *Renewable and Sustainable Energy Reviews*, vol. 113, p. 109252, Oct. 2019, doi: 10.1016/J.RSER.2019.109252.

[10] Z. Bai, Q. Liu, J. Lei, and H. Jin, “Investigation on the mid-temperature solar thermochemical power generation system with methanol decomposition,” *Appl Energy*, vol. 217, pp. 56–65, May 2018, doi: 10.1016/J.APENERGY.2018.02.101.

[11] S. Kuravi, J. Trahan, D. Y. Goswami, M. M. Rahman, and E. K. Stefanakos, “Thermal energy storage technologies and systems for concentrating solar power plants,” *Prog Energy Combust Sci*, vol. 39, no. 4, pp. 285–319, Aug. 2013, doi: 10.1016/J.PECS.2013.02.001.

[12] K. E. N’Tsoukpoe, H. Liu, N. Le Pierrès, and L. Luo, “A review on long-term sorption solar energy storage,” *Renewable and Sustainable Energy Reviews*, vol. 13, no. 9, pp. 2385–2396, Dec. 2009, doi: 10.1016/J.RSER.2009.05.008.

[13] S. Mukherjee, S. V. Devaguptapu, A. Sviripa, C. R. F. Lund, and G. Wu, “Low-temperature ammonia decomposition catalysts for hydrogen generation,” *Appl Catal B*, vol. 226, pp. 162–181, Jun. 2018, doi: 10.1016/J.APCATB.2017.12.039.

[14] A. Zarebska, D. Romero Nieto, K. v. Christensen, L. Fjerbæk Søtoft, and B. Norddahl, “Ammonium Fertilisers Production from Manure: A Critical Review,”

 https://doi.org/10.52202/069564-0199

http://dx.doi.org/10.1080/10643389.2014.955630, vol. 45, no. 14, pp. 1469–1521, Jul. 2015, doi: 10.1080/10643389.2014.955630.

[15] M. J. Palys, H. Wang, Q. Zhang, and P. Daoutidis, "Renewable ammonia for sustainable energy and agriculture: vision and systems engineering opportunities," *Curr Opin Chem Eng*, vol. 31, p. 100667, Mar. 2021, doi: 10.1016/J.COCHE.2020.100667.

[16] C. Xu *et al.*, "Thermodynamic analysis of a novel biomass polygeneration system for ammonia synthesis and power generation using Allam power cycle," *Energy Convers Manag*, vol. 247, p. 114746, Nov. 2021, doi: 10.1016/J.ENCONMAN.2021.114746.

[17] R. Michalsky and P. H. Pfromm, "Thermodynamics of metal reactants for ammonia synthesis from steam, nitrogen and biomass at atmospheric pressure," *AIChE Journal*, vol. 58, no. 10, pp. 3203–3213, Oct. 2012, doi: 10.1002/AIC.13717.

[18] H. Ishaq and I. Dincer, "A novel biomass gasification based cascaded hydrogen and ammonia synthesis system using Stoichiometric and Gibbs reactors," *Biomass Bioenergy*, vol. 145, p. 105929, Feb. 2021, doi: 10.1016/J.BIOMBIOE.2020.105929.

[19] C. Zhang *et al.*, "Mimicking πbackdonation in Ce-MOFs for Solar-Driven Ammonia Synthesis," *ACS Appl Mater Interfaces*, vol. 11, no. 33, pp. 29917–29923, Aug. 2019, doi: 10.1021/ACSAMI.9B08682/SUPPL_FILE/AM9B08682_SI_001.PDF.

[20] H. Li, J. Shang, J. Shi, K. Zhao, and L. Zhang, "Facet-dependent solar ammonia synthesis of BiOCl nanosheets via a proton-assisted electron transfer pathway," *Nanoscale*, vol. 8, no. 4, pp. 1986–1993, Jan. 2016, doi: 10.1039/C5NR07380D.

[21] M. Malmali, M. Reese, A. v. McCormick, and E. L. Cussler, "Converting Wind Energy to Ammonia at Lower Pressure," *ACS Sustain Chem Eng*, vol. 6, no. 1, pp. 827–834, Jan. 2018, doi: 10.1021/ACSSUSCHEMENG.7B03159/ASSET/IMAGES/MEDIUM/SC-2017-03159W_0008.GIF.

[22] K. Verleysen, D. Coppitters, A. Parente, W. de Paepe, and F. Contino, "How can power-to-ammonia be robust? Optimisation of an ammonia synthesis plant powered by a wind turbine considering operational uncertainties," *Fuel*, vol. 266, p. 117049, Apr. 2020, doi: 10.1016/J.FUEL.2020.117049.

[23] X. M. Guo, E. Trably, E. Latrille, H. Carrre, and J. P. Steyer, "Hydrogen production from agricultural waste by dark fermentation: A review," *Int J Hydrogen Energy*, vol. 35, no. 19, pp. 10660–10673, Oct. 2010, doi: 10.1016/J.IJHYDENE.2010.03.008.

[24] P. O. Carden, "Energy corradiation using the reversible ammonia reaction," *Solar Energy*, vol. 19, no. 4, pp. 365–378, Jan. 1977, doi: 10.1016/0038-092X(77)90008-1.

[25] K. Lovegrove, A. Luzzi, M. McCann, and O. Freitag, "EXERGY ANALYSIS OF AMMONIA-BASED SOLAR THERMOCHEMICAL POWER SYSTEMS," *Solar Energy*, vol. 66, no. 2, pp. 103–115, Jun. 1999, doi: 10.1016/S0038-092X(98)00132-7.

[26] C. Chen, Y. Liu, H. Aryafar, T. Wen, and A. S. Lavine, "Performance of conical ammonia dissociation reactors for solar thermochemical energy storage," *Appl Energy*, vol. 255, p. 113785, Dec. 2019, doi: 10.1016/J.APENERGY.2019.113785.

[27] H. Kreetz and K. Lovegrove, "Theoretical analysis and experimental results of a 1 kWchem ammonia synthesis reactor for a solar thermochemical energy storage system," *Solar Energy*, vol. 67, no. 4–6, pp. 287–296, Jan. 1999, doi: 10.1016/S0038-092X(00)00064-5.

[28] K. Lovegrove, A. Luzzi, and H. Kreetz, "A solar-driven ammonia-based thermochemical energy storage system," *Solar Energy*, vol. 67, no. 4–6, pp. 309–316, Jan. 1999, doi: 10.1016/S0038-092X(00)00074-8.

[29] H. Zhang, L. Wang, J. Van herle, F. Maréchal, and U. Desideri, "Techno-economic comparison of green ammonia production processes," *Appl Energy*, vol. 259, Feb. 2020, doi: 10.1016/j.apenergy.2019.114135.

[30] N. Campion, H. Nami, P. R. Swisher, P. Vang Hendriksen, and M. Münster, "Techno-economic assessment of green ammonia production with different wind and solar potentials," *Renewable and Sustainable Energy Reviews*, vol. 173, Mar. 2023, doi: 10.1016/j.rser.2022.113057.

[31] M. D. Mukelabai, J. M. Gillard, and K. Patchigolla, "A novel integration of a green power-to-ammonia to power system: Reversible solid oxide fuel cell for hydrogen and power production coupled with an ammonia synthesis unit," *Int J Hydrogen Energy*, vol. 46, no. 35, pp. 18546–18556, May 2021, doi: 10.1016/J.IJHYDENE.2021.02.218.

[32] A. S. Chellappa, C. M. Fischer, and W. J. Thomson, "Ammonia decomposition kinetics over Ni-Pt/Al 2 O 3 for PEM fuel cell applications," 2002.

[33] G. Masci, C. Ortiz, R. Chacartegui, V. Verda, and J. M. Valverde, "The ammonia looping system for mid-temperature thermochemical energy storage," *Chem Eng Trans*, vol. 70, pp. 763–768, 2018, doi: 10.3303/CET1870128.

[34] Y. Ohtsuka, C. Xu, D. Kong, and N. Tsubouchi, “Decomposition of ammonia with iron and calcium catalysts supported on coal chars,” *Fuel*, vol. 83, no. 6, pp. 685–692, Apr. 2004, doi: 10.1016/J.FUEL.2003.05.002.

[35] J. Humphreys, R. Lan, and S. Tao, “Development and Recent Progress on Ammonia Synthesis Catalysts for Haber–Bosch Process,” *Advanced Energy and Sustainability Research*, vol. 2, no. 1, p. 2000043, Jan. 2021, doi: 10.1002/aesr.202000043.

[36] H. Zhang, L. Wang, J. Van herle, F. Maréchal, and U. Desideri, “Techno-economic comparison of green ammonia production processes,” *Appl Energy*, vol. 259, p. 114135, Feb. 2020, doi: 10.1016/J.APENERGY.2019.114135.

[37] M. D. Carlson, B. M. Middleton, and C. K. Ho, “PowerEnergy2017-3590 TECHNO-ECONOMIC COMPARISON OF SOLAR-DRIVEN SCO2 BRAYTON CYCLES USING COMPONENT COST MODELS BASELINED WITH VENDOR DATA AND ESTIMATES.”

[38] U. Tesio, E. Guelpa, and V. Verda, “Integration of thermochemical energy storage in concentrated solar power. Part 1: Energy and economic analysis/optimisation,” *Energy Conversion and Management: X*, vol. 6, p. 100039, Apr. 2020, doi: 10.1016/J.ECMX.2020.100039.

[39] E. De Lena *et al.*, “Techno-economic analysis of calcium looping processes for low CO2 emission cement plants,” *International Journal of Greenhouse Gas Control*, vol. 82, pp. 244–260, Mar. 2019, doi: 10.1016/J.IJGGC.2019.01.005.

[40] A. Bayon *et al.*, “Techno-economic assessment of solid–gas thermochemical energy storage systems for solar thermal power applications,” *Energy*, vol. 149, pp. 473–484, Apr. 2018, doi: 10.1016/J.ENERGY.2017.11.084.

[41] C. K. Ho, “A review of high-temperature particle receivers for concentrating solar power,” *Appl Therm Eng*, vol. 109, pp. 958–969, Oct. 2016, doi: 10.1016/J.APPLTHERMALENG.2016.04.103.

[42] V. Jülch, “Comparison of electricity storage options using levelized cost of storage (LCOS) method,” *Appl Energy*, vol. 183, pp. 1594–1606, Dec. 2016, doi: 10.1016/j.apenergy.2016.08.165.

https://doi.org/10.52202/069564-0199